2022-06

Modeling nosocomial infection of COVID-19 transmission dynamics
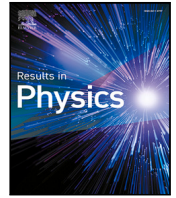
Masandawa, Lemjini

Provided with love from The Nelson Mandela African Institution of Science and Technology

Modeling nosocomial infection of COVID-19 transmission dynamics

Lemjini Masandawa [b,*], Silas Steven Mirau [b], Isambi Sailon Mbalawata [a], James Nicodemus Paul [b], Katharina Kreppel [b], Oscar M. Msamba [c]

[a] African Institute for Mathematical Sciences, NEI Globla Secretariat, Rue KG590 ST, Kigali, Rwanda
[b] School of Computational and Communication Science and Engineering, The Nelson Mandela African Institution of Science and Technology, P.O. Box 447, Arusha, Tanzania
[c] Arusha Technical College, P.O. Box 296, Arusha, Tanzania

ARTICLE INFO

ABSTRACT

COVID-19 epidemic has posed an unprecedented threat to global public health. The disease has alarmed the healthcare system with the harm of nosocomial infection. Nosocomial spread of COVID-19 has been discovered and reported globally in different healthcare facilities. Asymptomatic patients and super-spreaders are sough to be among of the source of these infections. Thus, this study contributes to the subject by formulating a $SEIHR$ mathematical model to gain the insight into nosocomial infection for COVID-19 transmission dynamics. The role of personal protective equipment θ is studied in the proposed model. Benefiting the next generation matrix method, R_0 was computed. Routh–Hurwitz criterion and stable Metzler matrix theory revealed that COVID-19-free equilibrium point is locally and globally asymptotically stable whenever $R_0 < 1$. Lyapunov function depicted that the endemic equilibrium point is globally asymptotically stable when $R_0 > 1$. Further, the dynamics behavior of R_0 was explored when varying θ. In the absence of θ, the value of R_0 was 8.4584 which implies the expansion of the disease. When θ is introduced in the model, R_0 was 0.4229, indicating the decrease of the disease in the community. Numerical solutions were simulated by using Runge–Kutta fourth-order method. Global sensitivity analysis is performed to present the most significant parameter. The numerical results illustrated mathematically that personal protective equipment can minimizes nosocomial infections of COVID-19.

Introduction

Recently, more attention has been given to the research of epidemic diseases like H1N1, malaria, Ebola, HIV, HBV, and many others [1]. The ability of bacteria, viruses, and parasites which are causative agents of these infectious diseases to keep changing over time posed challenges in controlling them. Currently the newest of the epidemic diseases disturbing the whole world is called COVID-19 [1]. COVID-19 is a respiratory illness that spread to many parts of the world within a short period after its evolution in China in late December in the year 2019 [2, 3]. It is the newest kind of virus caused by SARS COV-2 [4]. COVID-19 can affect either the lower respiratory tract (lungs and windpipes) or the upper respiratory tract (throat, sinuses, and nose). It started as unusual pneumonia of unknown etiology in Wuhan City in central China. On 7 January, 2020 it was discovered that the cause of the new outbreak of pneumonia is called the novel coronavirus (2019-nCOV) and later, on 11 February, 2020 the disease is named as Coronavirus Disease 2019 (COVID-19) [5]. Some studies suggested that the potential intermediary source of the novel infection is pangolins [3,6]. In spite

of the fact that the Chinese government imposed a strong lockdown, yet the disease spread very quickly throughout China and many other parts of the world through travelers from Wuhan. WHO announced it as pandemic on 11 March, 2020.

COVID-19 is transmitted from one person to another via breathing in the large respiration system's droplets coming from the mucous membrane (eye, mouth, and nose) of an infected person when sneezing, coughing, talking, or exhaling [7]. These respiratory droplets are too heavy to hang in the air so, the force of gravity influences and travel not more than one meter before quickly falling on the floor or surface thus, a social distance of 2 meters is a precaution. Further, the disease can be acquired through fomite transmission [8]. Predominantly transmission occurs through inhaling respiratory droplets from an infected person in close contact.

Zamir et al. [9] in their research presented that about 75% of COVID-19 victims do not show symptoms but recover naturally from the disease, only 20% can develop symptoms. The infected person will take 2–14 days to manifest full symptoms of the disease [10].

About 80% of infected individuals recover without any treatment [10]. Mid-infected individuals recover within two weeks while critical cases recover within 3 to 6 weeks. The mortality and recovery rate of the disease is 7% and 93%, respectively [11]

The disease is much severe to the age group of 65 and above compared to young people. The human population having a long-term illness that weakens the body immunity such as cancer, diabetes, hypertension, and cardiovascular have the highest chance of getting much sickness [7]. Common symptoms for the disease include tiredness, sleep disorders, throat infection, nausea, vomiting, diarrhea, severe headache, muscles ache, runny nose, dry cough, red eyes, fatigue, sneezing, losing smell, and test [10,12]. The very serious clinical symptoms include breathing problems, persistent pain in the chest, blood pressure, kidney failure, and lack of voluntary movement [13]

Basic reproduction number R_0 is the threshold parameter which can be used to govern the spread of a specific disease. It helps in knowing how many in average one sick person can infect. In regards to COVID-19, one study revealed that R_0 to be 6.33 which is the highest value in German during the early outbreak of the disease [14]. One of the study done in Africa evinced the value of R_0 to be 2.37 [15].

Theories and practices of mathematical models have a paramount importance in describing infectious diseases. Formulation and analysis of these models can assist to gain an insight about the mechanism for the spread as well as the characteristic of the disease. Mathematical models can provide an information which can be useful in suggesting an effective strategy for prediction and prevention of the disease in the population. To date, there are plenty of mathematical models for describing the transmission dynamics of COVID-19 [5,13,14,16–23].

Apart from the global impact of economic and social disruption caused by the novel coronavirus, it has alarmed the healthcare system with the harm of healthcare-associated infection (HAI) [24]. These infections are acquired from the hospital setting. These infections are spread by various means, including between co-healthcare workers, between public healthcare workers and patients, and between sick individuals themselves [25]. Medical staff can acquire or transmit disease indirectly when attending infected individuals or susceptible patients. Also, the spread of infections in hospitals from infected to healthy personal is through directly sharing of the same rooms and environments.

Different governments around the world have been discovering hospital-acquired infections for COVID-19 in their healthcare facilities and report. One research conducted in one of the hospital in Germany revealed a total of 48 COVID-19 confirmed cases associated with HAI, in which 28 were healthcare professionals (HCPs), and 7 were accompanying their family members to the hospital, and 13 were patients in the hospitals [24]. Out of aforementioned cases, 4 infected persons had a 15 minutes close interaction with medical staffs without wearing personal protective equipment (PPE). In addition, seven other HCPs became infected after provision of medication to COVID-19 sick individuals without wearing PPE [24]. The other study depicted that the prevalence of nosocomial infections for COVID-19 was between 12.5%–15% in the united kingdom and up to 44% in China [26].

One of the research conducted by Lecy-Schoenherr [27] revealed that, HAI can be prevented through proper wearing of PPE, appropriate hand hygiene, proper monitoring of sick persons, and regular disinfecting environments. Since the outset of the pandemic the resources such as goggles, masks, apron, gloves, and gowns collectively termed PPE have been in a limited supply [25,28]. There are few research done on nosocomial transmission of SARS-COV-2. Martos et al. [26] did modeling on the transmission dynamics of COVID-19 inside hospital bays, a research conducted in UK. Authors in their paper, they focused only on the hospitalized patients. Du et al. [24] in their review paper, reported nosocomial infections of SARS-COV-2 as new challenge to the healthcare professionals. In their work they suggested different strategies such as education, hygiene and environmental surveillance as means to prevent nosocomial infection. Oke et al. [29] formulated

a SEIHRD mathematical model to examine the impact of saturated treatment in Nigeria. In their study they concluded that minimization of infectivity rate alone cannot stop COVID-19 but can only be controlled when the disease's protocols are observed. Currently, little is known about the impact of PPE on COVID-19 nosocomial transmission dynamics.

Motivated by the above reason, the study at hand proposes a compartmental model to analyze the impact of PPE on nosocomial infection of the novel coronavirus transmission dynamics.

After introduction in the first part, the rest of the articles is designed as follows. The proposed model for COVID-19 nosocomial infection is presented in a section named "Mathematical Model Development and Description". In another part by the name "Analysis of the Proposed COVID-19 Model" of the paper, theoretical analysis is investigated. A section of "Numerical Simulation" presents the numerical simulations. Conclusions, and the future direction is presented in the last section.

Mathematical model development and description

Deterministic compartment models divided the population into groups which are defined by the possible disease states that could be there at a specific time. This is a basis for the foundation of mathematical epidemiology since it helps in building models. In the proposed deterministic model the available population is categorized into five classes such as: Susceptible individuals (S), Exposed individuals (E), Infected individuals (I), Hospitalized individuals (H) and Recovered individuals (R). Therefore

$$N(t) = S(t) + E(t) + I(t) + H(t) + R(t),$$

where $N(t)$ indicate the whole population. The flowchart of the model is depicted in Fig. 1. When building this deterministic model, the available population is assumed to mix freely. Also, we assumed since the chance that a random contact by an infective is with a susceptible, who can then transmit infection is $\frac{S}{N}$, therefore the rate of new infection is given as $\left(\frac{S}{N}\right)(\beta_1 I + \beta_2 H) N = (\beta_1 I + \beta_2 H)S$. The susceptible class is increased by birth at a rate of Λ and recovered individuals who soon lost their immunity at the rate of γ. A susceptible compartment may catch the infection after enough contact with I and H. In some circumstances, individuals who accompany their patients to health facilities may acquire the disease through their interaction with patients and sharing the same environments. Further, Medical staff can acquire or transmit disease indirectly when attending to infected individuals or susceptible patients. So, hospitalized individuals and public health workers are assumed to participate in disease transmission but at a lower rate compared to free-leaving infectious individuals. β_1 and β_2 present the coefficients of the disease transmission relative to both infected and hospitalized class, respectively. The proportion of individuals who wear PPE within the community is denoted as θ where $0 \leq \theta \leq 1$. Contact tracing and isolation of individuals into the hospital is done at the rate of ε. Self-isolated individuals enter into the compartment I at the transformation rate of α. Hospitalized individuals are assumed to be infectious but with a low infectivity rate compared to $I(t)$. Among hospitalized groups and active patients the death occurs at the rate of d. The infected individuals are admitted to the hospital when they suffer from advanced symptoms of COVID-19 such as shorten in a breath at the rate of ν, otherwise join the group of individuals who have recovered at the rate of δ after their bodies gaining natural immunity. Hospitalized cases are discharged from the hospital and join the recovered group with the rate of ω. Finally, the parameter μ represents death due to the novel coronavirus rate for all individuals in all five compartments.

In formulating the proposed model for this paper the following hypothesis are made:
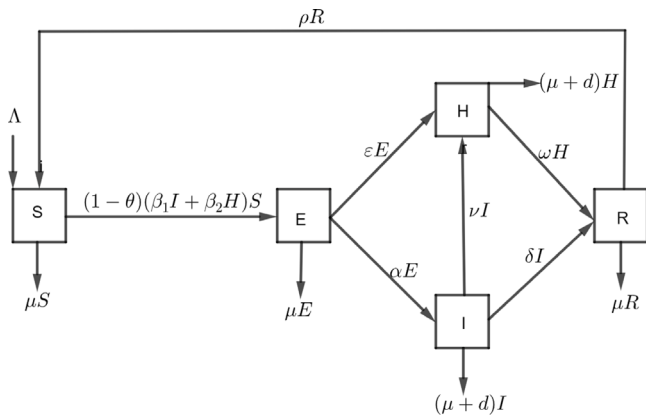
    i. All individuals are born susceptible.

Fig. 1. Schematic diagram of COVID-19.

Table 1
Model variable description.

Variables	Description
$N(t)$	Total population at given time t
$S(t)$	Susceptible population at time t
$E(t)$	Exposed population at a given time t
$I(t)$	Infected population at time t
$H(t)$	Hospitalized population at time t
$R(t)$	Removed population at time t

Table 2
Parameters of the proposed model.

Parameter	Description
Λ	Recruitment rate
β_1	Contact rate
β_2	Contact rate of hospitalized group
μ	Removal rate
α	Rate at which exposed individuals become infected
ε	Rate at which exposed individuals are isolated in hospitals
ν	The rate where infected individuals are being hospitalized
ω	Recovery rate of hospitalized population
δ	The rate at which infected individuals recover
ρ	Rate of leaving the recovered class
d	The disease induced death rate
θ	The rate wearing PPE

ii. Vertical transmission are ignored.

iii. Initially every person in the population is considered susceptible.

Schematic diagram found in Fig. 1 can be used to derive Eq. (1). The meaning of state variables for Eq. (1) are found in Table 1.

Deploying the given assumptions and variables, Eq. (1) is formulated having positive initial conditions

$$\frac{dS}{dt} = \Lambda + \rho R - (\mu + (1-\theta)(\beta_1 I + \beta_2 H))S,$$
$$\frac{dE}{dt} = ((1-\theta)(\beta_1 I + \beta_2 H)S - (\alpha + \mu + \varepsilon)E),$$
$$\frac{dI}{dt} = \alpha E - (\delta + \nu + d + \mu)I, \qquad (1)$$
$$\frac{dH}{dt} = \varepsilon E + \nu I - (d + \mu + \omega)H,$$
$$\frac{dR}{dt} = \delta I + \omega H - (\mu + \rho)R.$$

Table 2 depicts the meaning of all parameters used in Eq. (1).

Analysis of the proposed COVID-19 model

This section covers positiveness of the solution, biological invariant region, equilibria solution, basic reproduction number, local and global stability of the proposed model (1).

Positiveness of the model of the solution

In this sub-section we have proved that the proposed model (1) solutions are positive for all $t \geq 0$.

Theorem 1. *Assume that the model solution (1) starts Ω and remain in Ω for all time $t \geq 0$ and*

$$\Omega = \{S(t), E(t), I(t), H(t), R(t)\} \in \mathbb{R}^5_+ \geq 0.$$

Proof. In proving this theorem, let us deploy an approach used by [30], Let define $\Psi(t) = \{x(t) = 0$ and $(S(t), E(t), I(t), H(t), R(t)) \in \mathbb{R}^5_+ \geq 0\}$ $\forall \in x : \{S(t), E(t), I(t), H(t), R(t)\}$. Therefore, from Eq. (1), we have:

$$\frac{dS}{dt}\Big|\Phi(S) = \Lambda + \rho R \geq 0,$$
$$\frac{dE}{dt}\Big|\Phi(E) = ((1-\theta)(\beta_1 I + \beta_2 H)S) \geq 0,$$
$$\frac{dI}{dt}\Big|\Phi(I) = \alpha E \geq 0,$$
$$\frac{dH}{dt}\Big|\Phi(H) = \varepsilon E + \nu I \geq 0,$$
$$\frac{dR}{dt}\Big|\Phi(R) = \delta I + \omega H \geq 0.$$

Using the approach by [30] helped in completing the proof. $\square$

Biological feasible region

The proposed model of COVID-19 nosocomial infection is realistic when all states variable are bounded in a feasible region Γ if initial conditions are positive for all $t \geq 0$.

Theorem 2. *Let the solutions for Eq. (1) with positive initial condition are stated in the feasible region Γ where*

$$\Gamma = \{S(t), E(t), I(t), H(t), R(t)\} \in \mathbb{R}^5_+$$

for all positive t.

Proof. To evaluate this, first consider the whole population which is given as:

$$N(t) = S(t) + E(t) + I(t) + H(t) + R(t).$$

Differentiating with respect to t leads to:

$$\frac{dN}{dt} = \frac{dS}{dt} + \frac{dE}{dt} + \frac{dI}{dt} + \frac{dH}{dt} + \frac{dR}{dt}. \qquad (2)$$

Substitute Eq. (1) into Eq. (2), further simplification result into:

$$\frac{dN}{dt} = \Lambda - \mu(S + E + I + H + R) - (I + H)d. \qquad (3)$$

Substituting N to the sum of all five states variables in Eq. (3) leads to:

$$\frac{dN}{dt} = \Lambda - \mu N - (I + H)d. \qquad (4)$$

In absence of death due to novel coronavirus ($d = 0$) Eq. (4) reduces to:

$$\frac{dN}{dt} \leq \Lambda - \mu N. \qquad (5)$$

Integrating both sides Eq. (5) with its initial condition gives:

$$\int_{N(0)}^{N(t)} \frac{dN}{\Lambda - \mu N} \leq \int_0^t dt.$$

Which simplifies into:

$$N(t) \leq N_0 e^{-\mu t} + \frac{\Lambda}{\mu}(1 - e^{-\mu t}).$$

As $t \to \infty$ the population size, $N(t) \to \frac{\Lambda}{\mu}$ which implies that $0 \leq N \leq \frac{\Lambda}{\mu}$, so the feasible region is given by $\Gamma = \{S, E, I, H, R\} \in \mathbb{R}^5_+ : 0 \leq N(t) \leq \frac{\Lambda}{\mu}$. Hence, the proposed model is well posed mathematically and this completes the proof. $\square$

Equilibrium analysis of model (1)

In any dynamical system, the state at which the system does not vary with time is called equilibrium point. Whenever the system starts from equilibrium it will never change for all time. There are two equilibria which are disease-free and endemic. Let E_0 be the disease-free point and it is given as:

$$E_0 = \left(S^0, E^0, I^0, H^0, R^0\right) = \left(\frac{\Lambda}{\mu}, 0, 0, 0, 0\right).$$

Further, an endemic equilibrium point (F^*) is given by:

$$I^* = \frac{\varepsilon E^*}{d + \delta + \mu + \nu} > 0,$$

$$H^* = \frac{\alpha E^* + \nu I^*}{d + \mu + \omega} > 0,$$

$$E^* = \frac{(1 - \theta)S^*\left(\beta_2 H^* + \beta_1 I^*\right)}{\alpha + \mu + \epsilon} > 0,$$

$$R^* = \frac{\omega H^* + \delta I^*}{\mu + \rho} > 0,$$

$$S^* = \frac{\Lambda + \rho R^*}{-\beta_2 \theta H^* + \beta_2 H^* + \mu - \beta_1 \theta I^* + \beta_1 I^*} > 0.$$

After obtaining S^*, E^*, I^*, H^* and R^* we have to formulate a quadratic function in the format

$$F(E^*) = A(E^*)^2 + BE^* + C = 0,$$

where by in our case the value of A and B are as follows:

$$A = \frac{p_1 + p_2 p_3}{p_4}, \tag{6}$$

where

$$p_1 = d^2(\mu + \rho)(\alpha + \mu + \epsilon) + d(\alpha(\mu + \rho)(\delta + 2\mu + \nu) + \alpha\mu\omega + \delta\mu(\mu + \rho + \epsilon)$$
$$+ (\mu + \rho)(\mu + \epsilon)(2\mu + \nu + \omega)).$$

$$p_2 = \mu(\alpha(\delta + \mu + \nu)(\mu + \rho + \omega) + \delta(\mu + \omega)(\mu + \rho + \epsilon) + \rho\omega(\mu + \nu + \epsilon)$$
$$+ (\mu + \nu)(\mu + \rho)(\mu + \epsilon) + \omega(\mu + \nu)(\mu + \epsilon)).$$

$$p_3 = \beta_2(\nu(\alpha + \epsilon) + \alpha(\delta + d + \mu)) + \beta_1\epsilon(\omega + \mu + d),$$

and

$$p_4 = -\frac{\theta - 1}{(d + \mu + \omega)^2(\mu + \rho)(\nu + \delta + \mu + d)^2}.$$

$$B = \mu(\alpha + \mu + \epsilon) + \frac{(\theta - 1)\Lambda\left(\beta_2(\nu(\epsilon + \alpha) + \alpha(\delta + \mu + d)) + \beta_1\epsilon(d + \mu + \omega)\right)}{(d + \mu + \omega)(d + \delta + \mu + \nu)}. \tag{7}$$

We have used quadratic formula to obtain the value of E^* as follows

$$E^* = -B + \frac{\sqrt{B^2 - 4AC}}{2A},$$

where A and B are given in Eqs. (6) and (7), respectively while C is equal to zero in this case.

$$E^* = \frac{\mu(\alpha + \mu + \epsilon)\left(\frac{(\theta-1)\Lambda\left(\beta_1(-\epsilon)(d+\mu+\omega) - \beta_2(\nu(\alpha+\epsilon)+\alpha(d+\delta+\mu))\right)}{\mu(\alpha+\mu+\epsilon)(d+\mu+\omega)(d+\delta+\mu+\nu)} - 1\right)}{\frac{\mu r_2\left((1-\theta)\Lambda(\alpha+\mu+\epsilon)\left(\beta_2(\nu(\alpha+\epsilon)+\alpha(d+\delta+\mu))+\beta_1\epsilon(d+\mu+\omega)\right)\right)}{\Lambda(\mu(\alpha+\mu+\epsilon)(d+\mu+\omega)(d+\delta+\mu+\nu))} + r_1}. \tag{8}$$

By substituting

$$R_0 = -\frac{(\theta - 1)\Lambda(\epsilon + \alpha + \mu)\left(\beta_2(\nu(\alpha + \epsilon) + \alpha(d + \delta + \mu)) + \beta_1\epsilon(d + \mu + \omega)\right)}{\mu(\alpha + \mu + \epsilon)(d + \mu + \omega)(d + \delta + \mu + \nu)},$$

in Eq. (8) lead to:

$$E^* = \frac{\Lambda\mu(\alpha + \epsilon + \mu)(R_0 - 1)}{\Lambda r_1 + \mu r_2 R_0},$$

where r_1 and r_2 are given in Box I.

Hence, we can conclude that the endemic point exist if and only if $R_0 > 1$.

Threshold parameter R_0

It is scientific test used to estimate the number of cases. It is commonly know as basic reproduction number. R_0 governs the spread of diseases. The next generation matrix is benefited in calculating the value of R_0 [31]. Consider Eq. (9) in a process of deducing R_0 as:

$$\frac{dE}{dt} = ((1 - \theta)S(\beta_1 I + \beta_2 H) - (\alpha + \mu + \epsilon)E,$$
$$\frac{dI}{dt} = \varepsilon E - (\delta + \nu + d + \mu)I, \tag{9}$$
$$\frac{dH}{dt} = \alpha E + \nu I - (d + \mu + \omega)H.$$

To distinguish between new infection from other changes in the population, the system of Eq. (9) is modified and to be yield:

$$\frac{dx_i}{dt} = F_i(x) - V_i(x),$$

where x_i is a state variable that belongs to the transmitting compartment, F_i the rate of new infections in the compartment i, V_i the transfer of infections from one compartment to another.

$$F_i = \begin{pmatrix} f_1 \\ f_2 \\ f_3 \end{pmatrix} = \begin{pmatrix} (1 - \theta)\frac{\Lambda}{\mu}(\beta_1 I + \beta_2 H) \\ 0 \\ 0 \end{pmatrix}.$$

Partial derivatives of F_i with respect to E, I and H at DFE E_0.

$$F = \begin{pmatrix} \frac{dF_1}{dE}(E_0) & \frac{dF_1}{dI}(E_0) & \frac{dF_1}{dH}(E_0) \\ \frac{dF_2}{dE}(E_0) & \frac{dF_2}{dI}(E_0) & \frac{dF_2}{dH}(E_0) \\ \frac{dF_3}{dE}(E_0) & \frac{dF_3}{dI}(E_0) & \frac{dF_3}{dH}(E_0) \end{pmatrix},$$

and

$$F = \begin{pmatrix} 0 & \beta_1(1 - \theta)\frac{\Lambda}{\mu} & \beta_2(1 - \theta)\frac{\Lambda}{\mu} \\ 0 & 0 & 0 \\ 0 & 0 & 0 \end{pmatrix}.$$

Considering V_i yields:

$$V_i = \begin{pmatrix} (\alpha + \mu + \epsilon)E \\ -\varepsilon E + (\mu + d + \nu + \delta)I \\ (\omega + \mu + d)H - \alpha E - \nu I \end{pmatrix},$$

Partial derivatives with respect to E, I, H results to:

$$V = \begin{pmatrix} \alpha + \epsilon + \mu & 0 & 0 \\ -\varepsilon & \mu + \nu + d + \delta & 0 \\ -\alpha & -\nu & d + \mu + \omega \end{pmatrix}.$$

The inverse of V is given as:

$$V^{-1} = \begin{pmatrix} \frac{1}{\alpha+\epsilon+\mu} & 0 & 0 \\ \frac{\epsilon}{(\alpha+\epsilon+\mu)(d+\delta+\mu+\nu)} & \frac{1}{d+\delta+\nu+\mu} & 0 \\ \frac{\alpha\delta+\alpha\mu+\alpha\nu+\alpha d+\epsilon\nu}{(\alpha+\epsilon+\mu)(d+\mu+\omega)(d+\delta+\mu+\nu)} & \frac{\nu}{(d+\mu+\omega)(d+\delta+\mu+\nu)} & \frac{1}{d+\mu+\omega} \end{pmatrix}.$$

The product of two Jacobian matrices (F and V^{-1}) gives:

$$FV^{-1} = \begin{pmatrix} \frac{\beta_2(1-\theta)\Lambda(\alpha\nu+d\epsilon+\delta\epsilon+\epsilon\mu+\epsilon\nu)}{\mu(\alpha+\epsilon+\mu)(d+\mu+\omega)(d+\delta+\mu+\nu)} + \frac{\beta_1(1-\theta)\Lambda\alpha}{\mu(\alpha+\epsilon+\mu)(d+\delta+\mu+\nu)} & \omega_1 & \frac{\beta_2(1-\theta)\Lambda}{\mu(d+\mu+\omega)} \\ 0 & 0 & 0 \\ 0 & 0 & 0 \end{pmatrix},$$

where

$$\omega_1 = \frac{\beta_2(1 - \theta)\Lambda\nu}{\mu(d + \mu + \omega)(d + \delta + \mu + \nu)} + \frac{\beta_1(1 - \theta)\Lambda}{\mu(d + \delta + \mu + \nu)}.$$

Eigenvalues are given by:

$$\left\{0, 0, \frac{(1 - \theta)\Lambda\left(\beta_2(\alpha\nu + \epsilon(d + \delta + \mu + \nu)) + \alpha\beta_1(d + \mu + \omega)\right)}{\mu(\alpha + \epsilon + \mu)(d + \mu + \omega)(d + \delta + \mu + \nu)}\right\}.$$

So

$$R_0 = \rho(FV^{-1}) = max(\lambda_1, \lambda_2, \lambda_3).$$

$$r_1 = \frac{d^2(1-\theta)(\rho+\mu)(\varepsilon+\mu\alpha) + d(\alpha(\mu+\rho)(\delta+2\mu+\nu) + \alpha\mu\omega + \delta\mu(\mu+\rho+\varepsilon) + (\mu+\rho)(\mu+\varepsilon)(2\mu+\nu+\omega))}{(\mu+\rho)(d+\mu+\omega)^2(d+\delta+\mu+\nu)^2},$$

and

$$r_2 = \frac{\mu(\alpha(\delta+\mu+\nu)(\mu+\rho+\omega) + \delta(\mu+\omega)(\mu+\rho+\varepsilon) + \rho\omega(\mu+\nu+\varepsilon) + (\mu+\nu)(\mu+\rho)(\mu+\varepsilon) + \omega(\mu+\nu)(\mu+\varepsilon))}{(\mu+\rho)(d+\mu+\omega)(d+\delta+\mu+\nu)}.$$

Box I.

$$a_2 = \frac{\alpha\beta_2(1-\theta)\Lambda + \beta_1(1-\theta)\Lambda\varepsilon + \mu\left(\alpha(\delta+2\mu+\nu+\omega) + d^2 + d(2\alpha+\delta+4\mu+\nu+\omega+2\varepsilon) + 2\delta\mu + \delta\omega + \delta\varepsilon + 2\mu\nu + 2\mu\omega + 3\mu + \nu\omega + 2\mu\varepsilon + \nu\varepsilon + \omega\varepsilon\right)}{\mu}.$$

Box II.

Therefore

$$R_0 = \frac{(1-\theta)\Lambda\left(\beta_2(\alpha\nu+\varepsilon(d+\delta+\mu+\nu)) + \alpha\beta_1(d+\mu+\omega)\right)}{\mu(\alpha+\varepsilon+\mu)(d+\mu+\omega)(d+\delta+\mu+\nu)}.$$

Stability analysis of the model

In this sub-section the proposed model is analyzed at disease-free (both local and global) and endemic. Metzler matrix and Lyapunov function are deployed in proving local and global stability, respectively.

Local behavior of the model

Local behavior of the model is achieved whenever all eigenvalues of the Jacobian matrix of the proposed model (1) at disease-free have non-positive real parts. Let demonstrate this by utilizing the ideas as in [32].

Theorem 3. *COVID-19 free equilibrium,* $E_0 = \left(S^0, E^0, I^0, H^0, R^0\right) = \left(\frac{\Lambda}{\mu}, 0, 0, 0, 0\right)$ *is locally asymptotically stable if and only if* $R_0 < 1$.

Proof. Partial differentiation of Eq. (1) at E_0 results to a matrix of the form:

$$J_{DFE} = \begin{pmatrix} -\mu & 0 & \frac{\beta_1(\theta-1)\Lambda}{\mu} & \frac{\beta_2(\theta-1)\Lambda}{\mu} & \rho \\ 0 & -\alpha-\mu-\epsilon & \frac{\beta_1(\theta-1)\Lambda}{\mu} & \frac{\beta_2(\theta-1)\Lambda}{\mu} & 0 \\ 0 & \epsilon & -d-\delta-\mu-\nu & 0 & 0 \\ 0 & \alpha & \nu & -d-\mu-\omega & 0 \\ 0 & 0 & \delta & \omega & -\mu-\rho \end{pmatrix}. \tag{10}$$

From Eq. (10), we have two eigenvalues which are $\lambda_1 = -\mu$ and $\lambda_2 = -\mu - \rho$.

$$J_{DFE} = \begin{pmatrix} -\alpha-\mu-\epsilon & \frac{\beta_1(\theta-1)\Lambda}{\mu} & \frac{\beta_2(\theta-1)\Lambda}{\mu} \\ \epsilon & -d-\delta-\mu-\nu & 0 \\ \alpha & \nu & -d-\mu-\omega \end{pmatrix}. \tag{11}$$

Eq. (11) leads to the characteristic equation given as:

$$Z(\lambda) = \lambda^3 + a_1\lambda^2 + a_2\lambda + a_3, \tag{12}$$

where

$$a_1 = \alpha + 2d + \delta + 3\mu + \nu + \omega + \epsilon.$$

a_2 is given in Box II.

$$a_3 = (\alpha+\varepsilon+\mu)(d+\mu+\omega)(d+\delta+\mu+\nu)(d+2\mu+\nu+\omega)(1-R_0).$$

By utilizing Routh–Hurwitz criteria, the negative real root of Fig. 12 is only obtained if and only if $a_1 > 0, a_3 > 0$ and $a_1 a_2 > a_3$. In our case, a_1 is non negative since it is a summation of positive variables, but in order for a_3 to be positive, $1 - R_0$ must be non-negative which implies $R_0 < 1$. Consequently, the disease-free equilibrium point is locally asymptotically stable whenever $R_0 < 1$, otherwise unstable. □

Global behavior of the model at E_0

The global behavior of the proposed model (1) is investigated using an approach presented in [33]. In showing that the eradication of COVID-19 in the human population does not dependent on the initial size of infected cases, it is very important to prove that disease-free equilibrium is globally asymptotically stable whenever $R_0 < 1$ [34].

Theorem 4. *Whenever* $R_0 < 1$, *the proposed COVID-19 model posses the disease-free equilibrium point which is globally asymptotically stable.*

Proof. Let us constructing Lyapunov function of the model (1) by considering the equation of the form:

$$P(t) = S - S^0 \ln S + E + I + H + R.$$

Taking derivatives both side yield

$$\frac{P(t)}{dt} = \left(1 - \frac{S^0}{S}\right)\frac{dS}{dt} + \frac{dE}{dt} + \frac{dI}{dt} + \frac{dH}{dt} + \frac{dR}{dt}. \tag{13}$$

Combining Eq. (1) with Eq. (13) at E_0 leads to:

$$\frac{P(t)}{dt} = \left(1 - \frac{S^0}{S}\right)(\Lambda - \mu S),$$

at point E_0, $S^0 = \frac{\Lambda}{\mu}$, $\Lambda = \mu S^0$, hence

$$\frac{P(t)}{dt} = \left(1 - \frac{S^0}{S}\right)(\mu S^0 - \mu S),$$

further simplification result to:

$$\frac{P(t)}{dt} = \frac{-\mu(S - S^0)^2}{S}.$$

Therefore $\frac{P(t)}{dt} \leq 0$. Also, it can be observed that the largest invariant set of the model (1) is obtained whenever $S = S^0$. Hence by LaSalle Invariance Principle [35] at E_0 the model (1) is globally asymptotically stable for $R_0 < 1$ and this completes the proof. □

Global behavior at F^*

In order to investigate the global behavior of the model (1), consider the Lyapunov function V as used in [36] which is defined as:

$$V(S, E, I, H, R) = A_1(S - S^* lnS) + A_2(E - E^* lnE) + A_3(I - I^* lnI) +$$

$A_4(H - H^* ln H) + A_5(R - R^* ln R)$. The constants A_1, A_2, A_3, A_4, and A_5 are non negative.

$$\frac{dV}{dt} = \begin{cases} A_1(1 - \frac{S^*}{S})\frac{dS}{dt} + A_2(1 - \frac{E^*}{E})\frac{dE}{dt} \\ + A_3(1 - \frac{I^*}{I})\frac{dI}{dt} + A_4(1 - \frac{H^*}{H})\frac{dH}{dt} \\ + A_5(1 - \frac{R^*}{R})\frac{dR}{dt}. \end{cases} \quad (14)$$

Substituting Eq. (1) into Eq. (14) yields:

$$\frac{dV}{dt} = \begin{cases} A_1(1 - \frac{S^*}{S})\Lambda + \rho R - (\mu + (1 - \theta)(\beta_1 I + \beta_2 H))S) \\ + A_2(1 - \frac{E^*}{E})((1 - \theta)(\beta_1 I + \beta_2 H)S - (\alpha + \varepsilon + \mu)E) \\ + A_3(1 - \frac{I^*}{I})(\alpha E - (\delta + \nu + \mu + d)I) \\ + A_4(1 - \frac{H^*}{H})(\varepsilon E + \nu I - (d + \mu + \omega)H) \\ + A_5(1 - \frac{R^*}{R})(\delta I + \omega H - (\mu + \rho)R). \end{cases} \quad (15)$$

By subsisting the value of the following parameters in Eq. (14) yield to Fig. 15.

$$\Lambda = \mu S^* + (1 - \theta)(\beta_1 I^* + \beta_2 H^*)S^* - \rho R^*,$$
$$\nu + d + \mu + \delta = \frac{\alpha E^*}{I^*},$$
$$d + \mu + \omega = \frac{\nu I^* + \alpha E^*}{H^*},$$
$$\mu + \rho = \frac{\delta I^* + \omega H^*}{R^*},$$
$$\alpha + \mu + \varepsilon = \frac{(1 - \theta)(\beta_1 I^* + \beta_2 H^*)S^*}{E^*}.$$

$$\frac{dV}{dt} = \begin{cases} A_1(1 - \frac{S^*}{S})(\mu + (1 - \theta)(\beta_1 I^* + \beta_2 H^*)S^*) - \gamma R^* \\ + \rho R - (\mu + (1 - \theta)(\beta_1 I + \beta_2 H)S) \\ + A_2(1 - \frac{E^*}{E})((1 - \theta)(\beta_1 I + \beta_2 H)S - \frac{(1 - \theta)(\beta_1 I^* + \beta_2 H^*)S^*}{E^*}E) \\ + A_3(1 - \frac{I^*}{I})(\alpha E - (\frac{\alpha E^*}{I^*})I) \\ + A_4(1 - \frac{H^*}{H})(\varepsilon E + \nu I - \frac{\nu I^* + \varepsilon E^*}{H^*}H) \\ + A_5(1 - \frac{R^*}{R})(\delta I + \omega H - \frac{\delta I^* + \omega H^*}{R^*}R). \end{cases} \quad (16)$$

Solving for constant A_i with $i = 1, 2, \ldots, 5$ after simplification we have the following results:

$$\frac{dV}{dt} = \begin{cases} (1 - \theta)\beta_2 H^* S^*(2 - \frac{S^*}{S} + \frac{H}{H^*} - \frac{E}{E^*} - \frac{HSE^*}{H^*S^*E}) \\ + (1 - \theta)\beta_1 I^* S^*(2 - \frac{S^*}{S} + \frac{I}{I^*} - \frac{E}{E^*} - \frac{ISE^*}{I^*S^*E}) \\ + \mu S^*(2 - \frac{S^*}{S} - \frac{S}{S^*}) + \rho R^*(1 - \frac{S^*}{S} - \frac{R}{R^*} + \frac{RS^*}{R^*S}) \\ + \alpha E^*(1 + \frac{E}{E^*} - \frac{I}{I^*} - \frac{EI^*}{E^*I}) \\ + \varepsilon E^*(1 + \frac{E}{E^*} - \frac{H}{H^*} - \frac{EH^*}{E^*H}) \\ + \nu I^*(1 + \frac{I}{I^*} - \frac{H}{H^*} - \frac{IH^*}{I^*H}) \\ + \omega H^*(1 - \frac{R}{R^*} + \frac{H}{H^*} - \frac{HR^*}{H^*R}) \\ + \delta I^*(1 - \frac{R}{R^*} + \frac{I}{I^*} - \frac{IR^*}{I^*R}) \end{cases} \quad (17)$$

Since the arithmetic mean exceeds the geometric mean, the following inequalities hold:

$$\begin{aligned}
&(2 - \frac{S^*}{S} + \frac{H}{H^*} - \frac{E}{E^*} - \frac{HSE^*}{H^*S^*E}) \leq 0, \\
&(2 - \frac{S^*}{S} + \frac{I}{I^*} - \frac{E}{E^*} - \frac{ISE^*}{I^*S^*E}) \leq 0, \\
&(2 - \frac{S^*}{S} - \frac{S}{S^*}) \leq 0, \\
&(1 - \frac{S^*}{S} - \frac{R}{R^*} + \frac{RS^*}{R^*S}) \leq 0, \\
&(1 + \frac{E}{E^*} - \frac{I}{I^*} - \frac{EI^*}{E^*I}) \leq 0, \\
&(1 + \frac{E}{E^*} - \frac{H}{H^*} - \frac{EH^*}{E^*H}) \leq 0, \\
&(1 + \frac{I}{I^*} - \frac{H}{H^*} - \frac{IH^*}{I^*H}) \leq 0, \\
&(1 - \frac{R}{R^*} + \frac{H}{H^*} - \frac{HR^*}{H^*R}) \leq 0, \\
&(1 - \frac{R}{R^*} + \frac{I}{I^*} - \frac{IR^*}{I^*R}) \leq 0.
\end{aligned} \quad (18)$$

Since the arithmetic mean is greater than or equal to geometric mean, it follows that from Eq. (18) one can note that $\frac{dV}{dt} \leq 0$ whenever $R_0 > 1$. Therefore by using LaSalle Invariance principle [35], the system (1) have global asymptotically stable endemic equilibrium point for all $R_0 > 1$ and this completes the proof of Theorem 5.

Theorem 5. *The proposed model* (1) *posses a very unique endemic equilibrium point if* $R_0 > 1$ *otherwise unstable.*

Numerical simulation

This part aids in prediction numerically on stability of Eq. (1) through using the fourth-order Runge–Kutta scheme. Numerical experiments are investigated so as to verify analytical results. The baseline parameters for experiments of the proposed model is found Table 3. In addition, stability of the model numerically at endemic together with impact of some control parameters are investigated. Further, the study at hand explored sensitivity analysis. There are other numerical scheme such Adams–Bashforth–Moulton method, Eulers' method, and Milne method used by other authors for numerical simulation [13,15].

Sensitivity and uncertainty analysis

This is a technique deployed to examine the impact of every parameter in relation to the model output. Global sensitivity analysis in epidemiology is used to check uncertainty of each input parameter in relation to uncertainty of outcome. This methods quantify the influence whenever all input parameters are varied. PRCC determines the quantification level of uncertainty by just considering the specific problem [37]. The global sensitivity analysis technique employed in this study is called partial rank correlation coefficient (PRCC). The lowest and the highest values of PRCC are -1 and 1, respectively. Fig. 2 depicts bars which correspond to PRCC values at a instance. Also, the same figure indicates the layout of histograms for basic reproduction number. The bars are named using numbers. Every number corresponds to its parameter in the order as seen in Table 3. Parameters with positive influence against R_0 are Λ, β_1, ε, d, ω, α, δ, ν, and β_2. Any positive partial rank correlation coefficient influence positively to R_0 while the negative partial rank correlation has a negative influence against the value of R_0. In our case the parameters θ and μ have negative PRCC values which lead to the decrease in the value of R_0.

Through using the baseline parameters in Table 3 the value of basic reproduction number R_0 obtained is 3.2988. Also, when $\theta = 0$ while other parameters are kept as seen in Table 3, then the value of $R_0 = 8.4584$. When $\theta = 0.95$ the value of $R_0 = 0.4229$. Under this note, the wearing of PPE minimizes the COVID-19 infection. Fig. 3 depicts a positive association between R_0 and the parameter β_2 while Fig. 4 stipulates the negative correlation between R_0 and the parameter θ.

Table 3
Parameters value with source.

S/N	Parameter	Value (day^{-1})	Source
1	Λ	40	[14]
2	θ	0.61	[14]
3	β_1	0.54944	[38]
4	ε	0.3716	[11]
5	d	0.00011	[34]
6	μ	0.0008	[14]
7	ω	0.65	[14]
8	α	0.083	[39]
9	δ	0.2	[14]
10	ν	0.0833	[40]
11	β_2	0.05	[29]

Fig. 2. Partial rank correlation coefficient (PRCC).

Fig. 3. Influence of β_2 on R_0.

Dynamics of human populations

Stability of the model (1) is investigated numerically by varying initial population. Fig. 5 evinces five sub-population with an initial condition such as $S(0) = 1000, E(0) = 70, I(0) = 40, H(0) = 30$ and $R(0) = 20$. The susceptible sub-population starts at 1000 and decay exponentially till the point of equilibrium. The recovered sub-population grow exponential and start maintaining its equilibrium point at around

Fig. 4. Influence of θ on R_0.

Fig. 5. Dynamics of $SWEI_sI_a HR$ sub-populations.

fifteen (15) days. The rest sub-population depicted by Fig. 5 describe the parabolic shape in the process of attaining equilibrium point.

Simulation on stability of Endemic Equilibrium Point (EEP)

We scrutinized the global stability at the endemic equilibrium point of the model system (1). The global stability can be attained whenever the model's state variables coming from distinguished initial values, varied for sometimes, convergence appeared in attaining the unique endemic numerical solution . The convergence of the model's trajectories to a common horizontal line signifies the global stability of the model system (1). Fig. 6 denotes five different trajectories originating from different assumed sub-population of the susceptible compartment such as S(0) = 1000, S(0) = 900, S(0) = 800, S(0) = 700 and S(0) = 600. All five trajectories converged to a common straight line after around eleven days. Figs. 7–9 depict the same results as the one stipulated in Fig. 6.

Impact of control parameters on the model

This part presents the numerical results of the model (1) when varying parameters θ, ω, and δ. Variation of aforementioned parameters
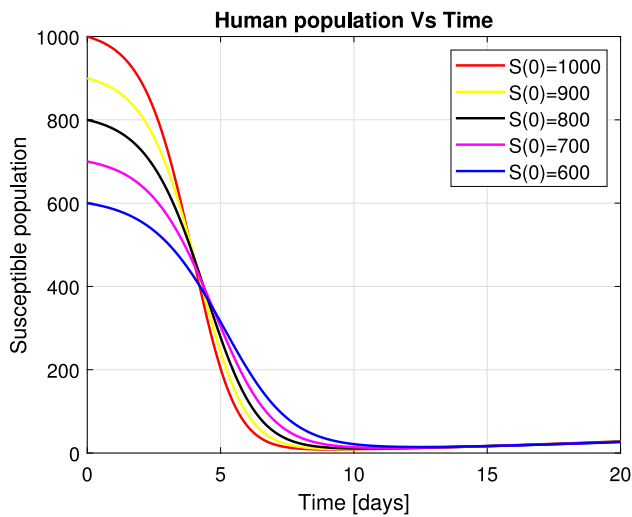
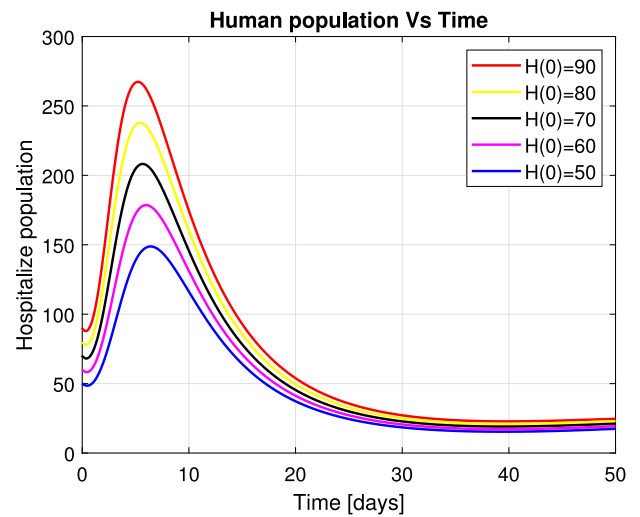**Fig. 6.** Stability of the EEP for susceptible human population.

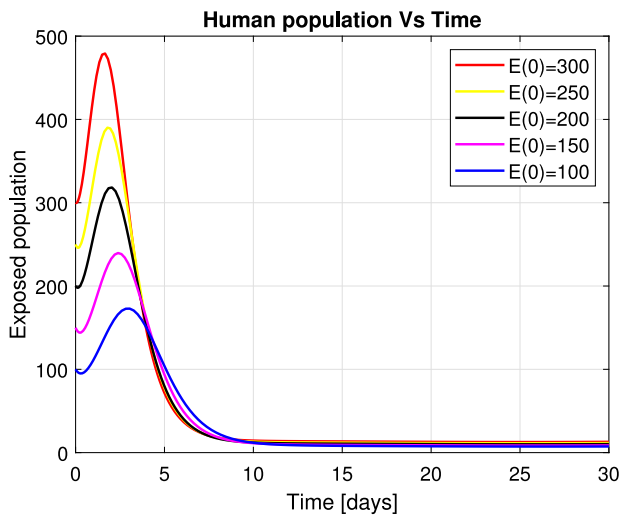**Fig. 7.** Stability of the EEP for exposed human population.
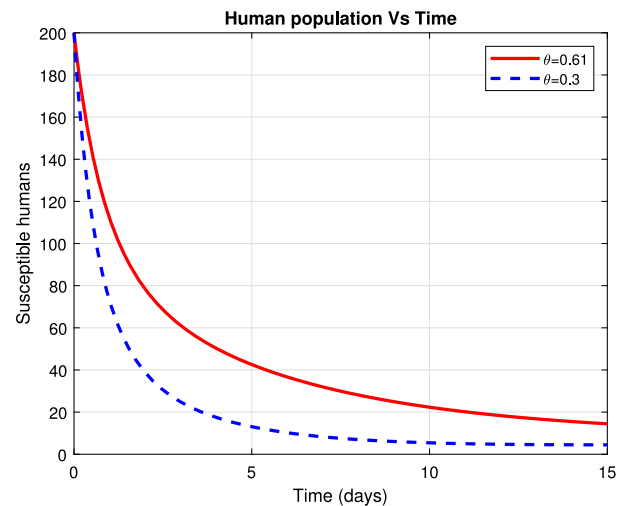
Fig. 8. Profile for stability of the EEP of infected human population.

Fig. 9. Profile for stability of the EEP of hospitalized human population.

Fig. 10. Influence of θ on susceptible population.

as observed in Table 3 aids in obtaining different graphical results for all state variables.

Fig. 10 shows the effect of use of PPE. Implementation PPE at a rate 0.61 helped a susceptible population to grow to around 15 individuals. Fig. 11 reveals that when PPE are worn at a rate of 0.61, exposed population reduces to about 66 individuals within only 10 days. Fig. 12 depicts the decrease in hospitalized patients to about 49 people due treatment given in the medical facilities as implemented at 65%. Fig. 13 evinces the grow of the number of the recovered population to about 447 individuals because of provision of medication in health facilities.

Fig. 14 depicts that the number of people who have recovered through acquiring natural body immunity at a rate of 0.2 is about 494. Fig. 15 shows that when θ is applied at 0.61 then the number infected individuals reduces to around 53 patients.

Discussion

The transmission dynamics of nosocomial infection for COVID-19 using a deterministic model was investigated. The parameter θ quantify the level of protection of the susceptible population when exposed to the disease. Figs. 10, 11 and 15 depicted that θ has a greater significance in reducing the spread of COVID-19 within human population. The numerical solutions obtained validated analytical results.
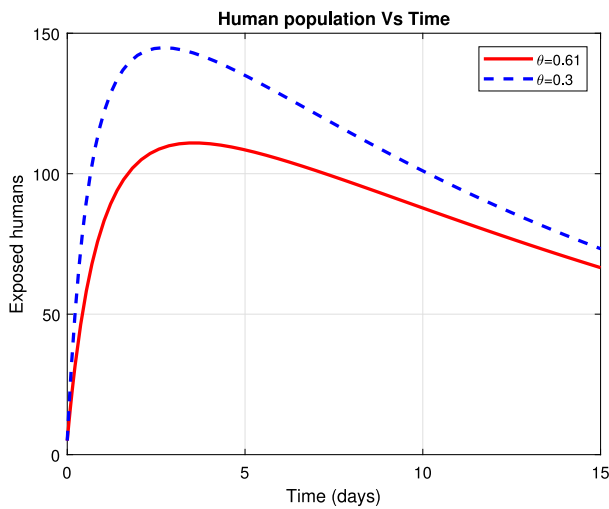
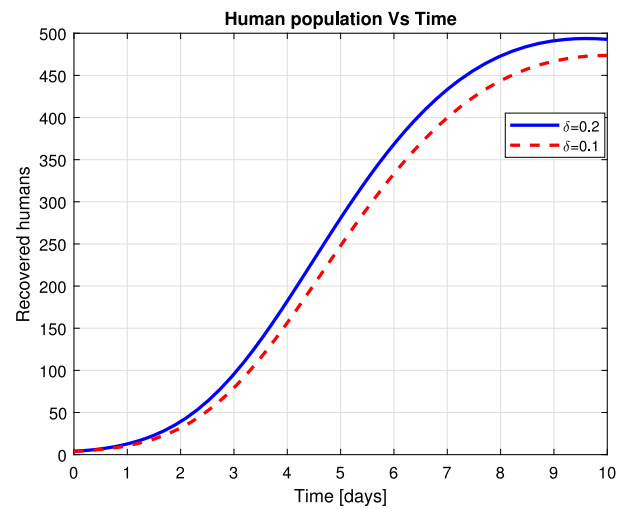**Fig. 11.** Influence of θ on exposed population.

Fig. 14. Effect of treatment (δ) recovered population.
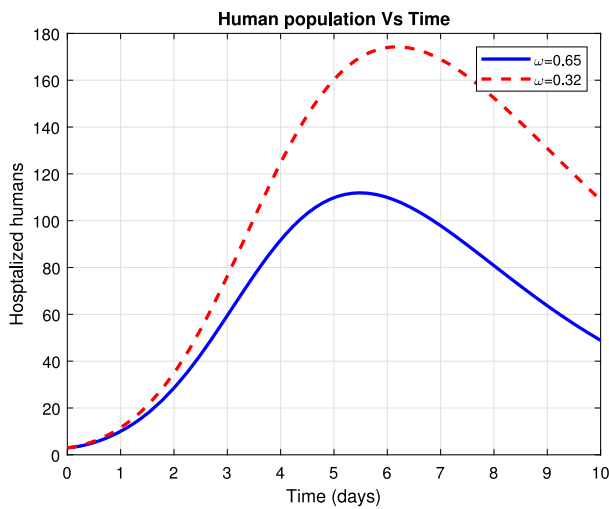

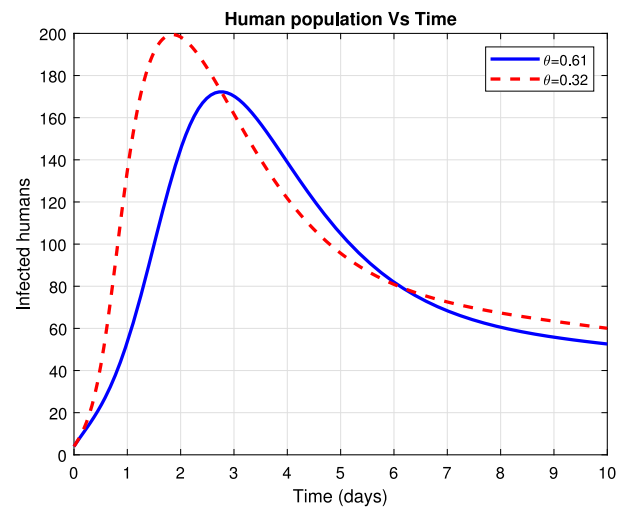**Fig. 12.** Effect of ω on hospitalized humans.

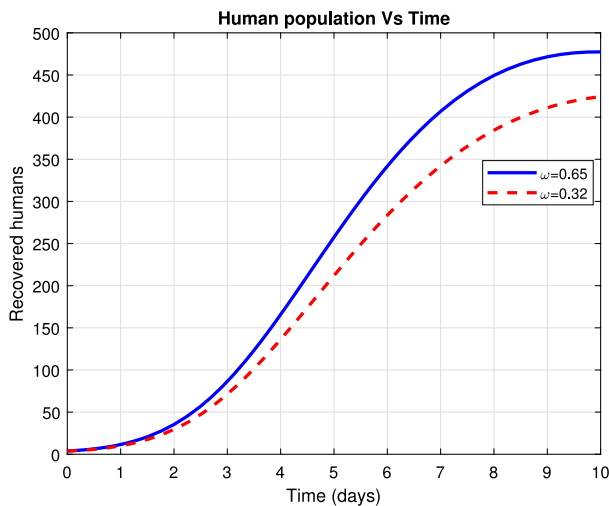**Fig. 15.** Effect of θ on infected humans.

Fig. 13. Effect of ω on recovered humans.

The stability of model (1) numerically is presented in Figs. 5 and 6–9. Positive and negative association between β_2, θ and R_0 are shown in Figs. 3 and 4, respectively.

Conclusion

This research work proposed a deterministic model for COVID-19 nosocomial infection which was used to scrutinize the effect of personal protective equipment in reducing the load of infections. We presented the detailed analysis of the model. Positivity and boundedness of the solution have been determined through calculus technique. Further, we computed the threshold quantity by benefiting the next generation matrix. By using Metzler matrix and linearization technique the disease-free equilibrium point is found to be locally and globally asymptotically stable whenever $R_0 < 1$. Through using Lyapunov function in combination with LaSalle's Invariance Principle the endemic equilibrium point is found to be globally asymptotically stable when $R_0 > 1$. The proposed model is solved numerically by using fourth-order Runge–Kutta scheme [41] and the numerical solutions depicted that if the parameter θ is absence in the proposed model, the threshold parameter value was 8.4584. However, when the parameter is rated to be 95% the threshold parameter value decrease to around 0.4229. Hence parameter θ seem to be capable in minimization of the spread of COVID-19.

Conclusively, the model solution revealed that transmission noso-comial infection of COVID-19 can be minimized in the community through effective use personal protective equipment.

The study should be modified to Caputo fractional derivatives model for the purpose of capturing more biological phenomena such as crossover behavior and fade memory [1,42]. Further, in near future real data will be used to fit the model for the purposes of parameter estimation. The study is limited with an assumption that the total population was uniformly distributed.

CRediT authorship contribution statement

Lemjini Masandawa: Conceptualization, Formal analysis, Model formulation, Software, Data curation, Writing – original draft, Methodology, Writing – review & eediting. **Silas Steven Mirau:** Supervision, Editing, Project administration. **Isambi Sailon Mbalawata:** Supervision, Editing, Project administration. **James Nicodemus Paul:** Supervision, Editing, Project administration. **Katharina Kreppel:** Supervision, Editing, Project administration. **Oscar M. Msamba:** Supervision, Editing, Project administration.

Declaration of competing interest

The authors declare that they have no known competing financial interests or personal relationships that could have appeared to influence the work reported in this paper.

Funding

References

[1] Naik PA, Yavuz M, Qureshi S, Zu J, Townley S. Modeling and analysis of COVID-19 epidemics with treatment in fractional derivatives using real data from Pakistan. Eur Phys J Plus 2020;135(10):1–42.

[2] Oud MAA, Ali A, Alrabaiah H, Ullah S, Khan MA, Islam S. A fractional order mathematical model for COVID-19 dynamics with quarantine, isolation, and environmental viral load. Adv Difference Equ 2021;2021(1):1–19.

[3] Mahmoudi MR, Heydari MH, Qasem SN, Mosavi A, Band SS. Principal component analysis to study the relations between the spread rates of COVID-19 in high risks countries. Alexandria Eng J 2021;60(1):457–64.

[4] Ivorra B, Ferrández MR, Vela-Pérez M, Ramos AM. Mathematical modeling of the spread of the coronavirus disease 2019 (COVID-19) taking into account the undetected infections. The case of China. Commun Nonlinear Sci Numer Simul 2020;88:105303.

[5] Abioye AI, Peter OJ, Ogunseye HA, Oguntolu FA, Oshinubi K, Ibrahim AA, Khan I. Mathematical model of covid-19 in nigeria with optimal control. Results Phys 2021;28:104598.

[6] Shayak B, Sharma MM, Rand RH, Singh AK, Misra A. Transmission dynamics of COVID-19 and impact on public health policy. MedRxiv 2020.

[7] Peter OJ, Qureshi S, Yusuf A, Al-Shomrani M, Idowu AA. A new mathematical model of COVID-19 using real data from Pakistan. Results Phys 2021;104098.

[8] Mbogo RW, Odhiambo JW. COVID-19 Outbreak, social distancing and mass testing in Kenya-insights from a mathematical model. Afrika Mat 2021;1–16.

[9] Zamir M, Nadeem F, Abdeljawad T, Hammouch Z. Threshold condition and non pharmaceutical interventions's control strategies for elimination of COVID-19. Results Phys 2021;20:103698.

[10] Ahmad W, Abbas M, Rafiq M, Baleanu D. Mathematical analysis for the effect of voluntary vaccination on the propagation of corona virus pandemic. Results Phys 2021;104917.

[11] Ali A, Alshammari FS, Islam S, Khan MA, Ullah S. Modeling and analysis of the dynamics of novel coronavirus (COVID-19) with Caputo fractional derivative. Results Phys 2021;20:103669.

[12] Gostic K, Gomez ACR, Mummah RO, Kucharski AJ, Lloyd-Smith JO. Estimated effectiveness of symptom and risk screening to prevent the spread of COVID-19. Elife 2020;9:e55570.

[13] Baba IA, Yusuf A, Nisar KS, Abdel-Aty A-H, Nofal TA. Mathematical model to assess the imposition of lockdown during COVID-19 pandemic. Results Phys 2021;20:103716.

[14] Masandawa L, Mirau SS, Mbalawata IS. Mathematical modeling of COVID-19 transmission dynamics between healthcare workers and community. Results Phys 2021;29:104731.

[15] Yu C-J, Wang Z-X, Xu Y, Hu M-X, Chen K, Qin G. Assessment of basic reproductive number for COVID-19 at global level: A meta-analysis. Medicine 2021;100(18).

[16] Gebremeskel AA, Berhe HW, Atsbaha HA. Mathematical modelling and analysis of COVID-19 epidemic and predicting its future situation in ethiopia. Results Phys 2021;22:103853.

[17] Ahmed I, Modu GU, Yusuf A, Kumam P, Yusuf I. A mathematical model of coronavirus disease (COVID-19) containing asymptomatic and symptomatic classes. Results Phys 2021;21:103776.

[18] Naik PA, Zu J, Ghori MB, et al. Modeling the effects of the contaminated environments on COVID-19 transmission in India. Results Phys 2021;29:104774.

[19] Abdulwasaa MA, Abdo MS, Shah K, Nofal TA, Panchal SK, Kawale SV, Abdel-Aty A-H. Fractal-fractional mathematical modeling and forecasting of new cases and deaths of COVID-19 epidemic outbreaks in India. Results Phys 2021;20:103702.

[20] Moore S, Hill EM, Tildesley MJ, Dyson L, Keeling MJ. Vaccination and non-pharmaceutical interventions for COVID-19: a mathematical modelling study. Lancet Infect Dis 2021.

[21] Redhwan SS, Abdo MS, Shah K, Abdeljawad T, Dawood S, Abdo HA, Shaikh SL. Mathematical modeling for the outbreak of the coronavirus (COVID-19) under fractional nonlocal operator. Results Phys 2020;19:103610.

[22] Zhang L, Ullah S, Al Alwan B, Alshehri A, Sumelka W. Mathematical assessment of constant and time-dependent control measures on the dynamics of the novel coronavirus: An application of optimal control theory. Results Phys 2021;104971.

[23] Atangana A, Araz SÍ. Mathematical model of COVID-19 spread in Turkey and South Africa: theory, methods, and applications. Adv Difference Equ 2020;2020(1):1–89.

[24] Du Q, Zhang D, Hu W, Li X, Xia Q, Wen T, Jia H. Nosocomial infection of COVID-19: A new challenge for healthcare professionals. Int J Mol Med 2021;47(4):1.

[25] Park Y, Sylla I, Das AK, Codella J. Agent-based modeling to evaluate nosocomial COVID-19 infections and related policies. Nature 2021;3:4.

[26] Martos DM, Parcell B, Eftimie R. Modelling the transmission of infectious diseases inside hospital bays: implications for COVID-19. MedRxiv 2020.

[27] Lecy-Schoenherr M. How the COVID-19 pandemic may have impacted hospital acquired infection rates. 2021.

[28] Pham TM, Tahir H, van de Wijgert JHHM, Van der Roest B, Ellerbroek P, Bonten MJM, Bootsma MCJ, Kretzschmar ME. Interventions to control nosocomial transmission of SARS-CoV-2: a modelling study. MedRxiv 2021.

[29] Oke II, Oyebo YT, Fakoya OF, Benson VS, Tunde YT. A mathematical model for Covid-19 disease transmission dynamics with impact of saturated treatment: Modeling, analysis and simulation. Open Access Libr J 2021;8(5):1–20.

[30] Asamoah JKK, Bornaa CS, Seidu B, Jin Z. Mathematical analysis of the effects of controls on transmission dynamics of SARS-CoV-2. Alexandria Eng J 2020;59(6):5069–78.

[31] Van den Driessche P, Watmough J. Reproduction numbers and sub-threshold endemic equilibria for compartmental models of disease transmission. Math Biosci 2002;180(1–2):29–48.

[32] Patil A. Routh-hurwitz criterion for stability: An overview and its implementation on characteristic equation vectors using MATLAB. Emerg Technol Data Min Inf Secur 2021;319–29.

[33] Syafruddin S, Noorani MSM. Lyapunov Function of SIR and SEIR model for transmission of dengue fever disease. Int J Simul Process Model 2013;8(2–3):177–84.

[34] Deressa CT, Duressa GF. Modeling and optimal control analysis of transmission dynamics of COVID-19: The case of ethiopia. Alexandria Eng J 2021;60(1):719–32.

[35] LaSalle JP. Stability theory and invariance principles. In: Dynamical systems. Elsevier; 1976, p. 211–22.

[36] Korobeinikov A, Wake GC. Lyapunov Functions and global stability for SIR, SIRS, and SIS epidemiological models. Appl Math Lett 2002;15(8):955–60.

[37] Marino S, Hogue IB, Ray CJ, Kirschner DE. A methodology for performing global uncertainty and sensitivity analysis in systems biology. J Theoret Biol 2008;254(1):178–96.

[38] Mugisha JYT, Ssebuliba J, Nakakawa JN, Kikawa CR, Ssematimba A. Mathematical modeling of COVID-19 transmission dynamics in Uganda: Implications of complacency and early easing of lockdown. PLoS One 2021;16(2):e0247456.

[39] Aldila D. Analyzing the impact of the media campaign and rapid testing for COVID-19 as an optimal control problem in East Java, Indonesia. Chaos Solitons Fractals 2020;141:110364.

[40] Diagne ML, Rwezaura H, Tchoumi SY, Tchuenche JM. A mathematical model of COVID-19 with vaccination and treatment. Comput Math Methods Med 2021;2021.

[41] Yavuz M, Coşar FO, Günay F, Özdemir FN. A new mathematical modeling of the COVID-19 pandemic including the vaccination campaign. Open J Model Simul 2021;9(3):299–321.

[42] Ali Z, Rabiei F, Shah K, Khodadadi T. Qualitative analysis of fractal-fractional order COVID-19 mathematical model with case study of Wuhan. Alexandria Eng J 2021;60(1):477–89.